SANS Data Fitting

Susana Teixeira[1,2]

[1]NIST Center for Neutron Research, National Inst. Standards and Technology, 100 Bureau Drive, Gaithersburg, MD 20899. [2]Dep. Chem. Biomolecular Engineering, U. Delaware, 150 Academy Str., Newark, DE 19716.

1. Introduction

The structure of lysozyme was the first ever solved for an enzyme [1]. Lysozymes are ubiquitous in mammalian tissues, and are present in phagocyte-like cells in nonmammalian organisms as well. There are three dominant families of lysozymes with different structure and activities: chicken-type (c-type), goose-type (g-type) and invertebrate-type (i-type). Generally, both c- and g-lysozymes are basic proteins due to their high isoelectric point (pI) values. c-Lysozyme is a single chain of 129 amino acids (14.3 kDa) that folds into a globular structure containing 4 α-helices and 5 β-strands, stabilized by 4 disulfide bridges. The enzyme is able to lyse peptidoglycan in the bacterial cell wall (see Figure 1), as well as act synergistically with other antimicrobial polypeptides.

(HEWL) is extensively used in food due to its abundant availability and properties. The electrostatic charge distribution of HEWL (calculated pI=9.28 [2]), with 9 negatively charged and 17 positively charged residues, imparts important binding affinities (see for example [3, 4]). There is extensive ongoing research towards improving the inhibitory effects of HEWL, relevant to its antimicrobial applications, namely through the formation of protein gels or complexes with other compounds (for a review see for example [5]). Further developments require systematic studies under different conditions environments – pressure [6], pH, salts, etc .

2. Sample and experimental data information

HEWL was obtained from Sigma (L-4919) and used without further purification. Two stock solutions of 150 mg/mL lysozyme were prepared in (A) D_2O and (B) 150 mM NaCl and D_2O. Dilutions of the stock solutions produced two samples for each of the two buffers, namely in the absence (A) and presence (B) of salt, as described in Table I. All samples were degassed prior to data collection. Sample concentrations were confirmed by measuring UV absorption at 280 nm (theoretical extinction coefficient 38940 M^{-1} cm^{-1}). For higher concentration samples (100 mg/mL), data were collected using 1 mm-thick cuvettes, while for the 1 mg/mL concentrations the samples were loaded in 2 mm-thick cuvettes. SANS data were collected for all samples at 25°C, using the NG7SANS 30m instrument of the NIST Center for Neutron Research [7] and a neutron wavelength of 6 Å ($\Delta\lambda/\lambda$ = 12.5%). Three sample-to-detector distances were used to cover a q-range of 0.003 – 0.55 $Å^{-1}$. Scattered intensities were recorded in a 640 mm x 640 mm ^{3}He position-sensitive proportional counter detector, with a 5.08 mm x 5.08 mm resolution.

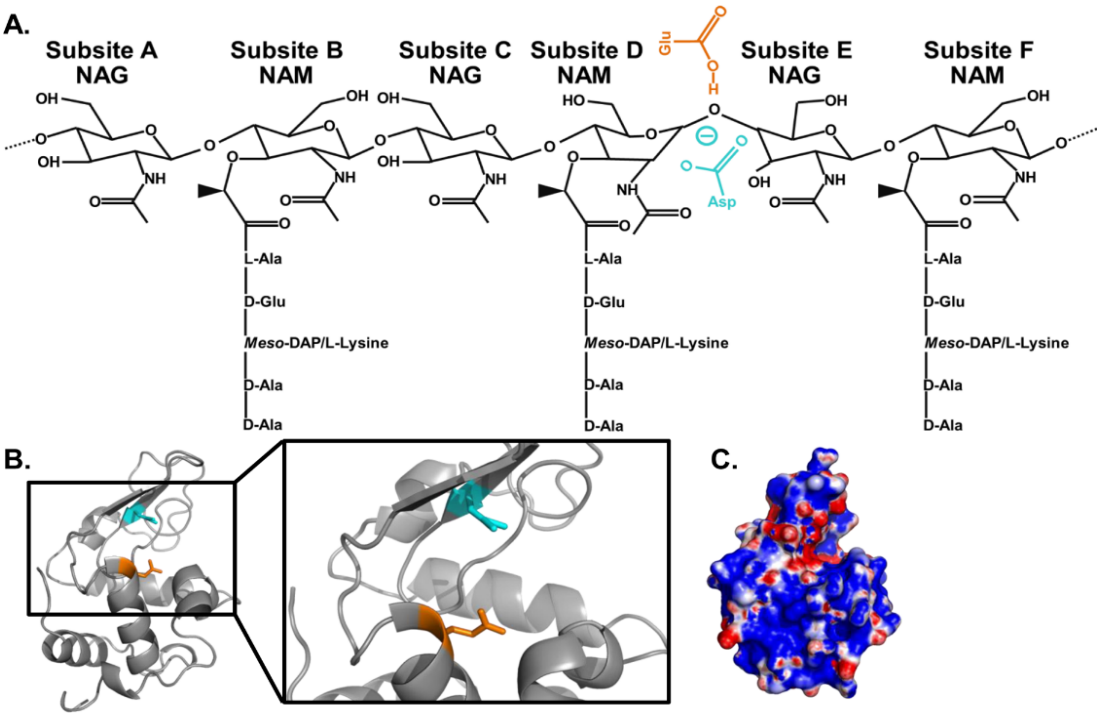

Figure 1. The enzymology and charge distribution of human lysozyme (PDB ID 1REX). **(A)** The active site accommodates up to 6 consecutive sugars annotated A-F. Lysozyme hydrolyzes the β-1,4 glycosidic bond between the subsite D and the subsite E. **(B)** Ribbon model of human lysozyme highlighting the essential active site residues in blue and orange. **(C)** Electrostatic potential map of human lysozyme, contoured at ± 5kT/e; blue, positive; red, negative; white, hydrophobic). Abbreviations: NAG, *N*-acetylglucosamine; NAM, *N*-acetylmuramic acid; PDB, Protein Data Bank. Image source: Ragland and Criss (2017) [8].

Table I. Sample formulations. The sample pH was measured before degassing.

Expected [Lysozyme] mg/mL		Measured [Lysozyme] mg/mL (A_{280})	Measured pD
Buffer A	0	0	6.8
	1.0	1.0	5.8
	100.0	101.0	4.5
Buffer B	0	0	5.3
	1.0	1.0	5.1
	100.0	99.8	4.3

3. Data fitting (dilute solutions): Form factors

All data analysis will be conducted using SasView, a freely-available small-angle scattering analysis software package [9]. Load the reduced and background-subtracted data for the dilute samples into

SasView. For this exercise, the dilute samples are assumed to be those that do not obviously show an interaction peak due to contribution from $S(q)$: 1.0 mg/mL data for both series A and B. Fit the data to a model using an ellipsoidal form factor (see Figure 2) $P(q)$ assuming $S(q) \approx 1$. This will provide the parameters for the ellipsoid.

Figure 2. Illustration adapted from [10], showing the approximate shape of the lysozyme molecule (PDB code 2LYZ) with a polar radius of ≈ 23 Å and an equatorial radius ≈ 12Å.

4. Data fitting: Structure factors

You will fit both the 1mg/mL and 100.0 mg/mL data from both Series A and Series B, with the corresponding ellipsoid parameters fixed, to obtain $S(q)$. Plot the fitted $S(q)$ curves for each sample on the same graph to compare the effects of concentration and the presence of salt in the buffer. You will be using a Hayter-Penfold Rescaled Mean Spherical Approximation (RMSA) structure factor for charged spheres [11], which calculates the interparticle structure factor for a system of charged, spheroidal, objects in a dielectric medium. This S(q) allows for inclusion of the interparticle interference effects due to screened Coulombic repulsion between the charged particles.

5. Discussion: suggested questions

A. Why are the fitted volume fractions less than 0.1 for the 100 mg/mL data?
B. What would be a better choice for the structure factor for the higher concentration data in 150 mM NaCl, where both attractive and repulsive forces could be in play?
C. Why didn't we choose the hard sphere structure factor for the 0 mM NaCl case?

Acknowledgements

The SANS tutorial benefited from the use of the SasView application, originally developed under NSF award DMR-0520547. SasView contains code developed with funding from the European Union's

Horizon 2020 research and innovation program under the SINE2020 project, grant agreement No 654000.

Disclaimer

Certain commercial equipment, instruments, suppliers are identified to foster understanding. This does not imply recommendation or endorsement by the National Institute of Standards and Technology, nor does it imply that the materials or equipment identified are necessarily the best available for the purpose.

REFERENCES

[1] L.N. Johnson, The early history of lysozyme, Nature Structural Biology 5(11) (1998) 942-944.

[2] M.R. Wilkins, E. Gasteiger, A. Bairoch, J.C. Sanchez, K.L. Williams, R.D. Appel, D.F. Hochstrasser, Protein identification and analysis tools in the ExPASy server, Methods Mol Biol 112 (1999) 531-52.

[3] A. Bijelic, C. Molitor, S.G. Mauracher, R. Al-Oweini, U. Kortz, A. Rompel, Hen egg-white lysozyme crystallisation: protein stacking and structure stability enhanced by a Tellurium(VI)-centred polyoxotungstate, Chembiochem 16(2) (2015) 233-41.

[4] M. Zaman, H.A. Safdari, A.N. Khan, S.M. Zakariya, S. Nusrat, T.I. Chandel, R.H. Khan, Interaction of anticancer drug pinostrobin with lysozyme: a biophysical and molecular docking approach, J Biomol Struct Dyn 37(16) (2019) 4338-4344.

[5] T. Wu, Q. Jiang, D. Wu, Y. Hu, S. Chen, T. Ding, X. Ye, D. Liu, J. Chen, What is new in lysozyme research and its application in food industry? A review, Food Chemistry 274 (2019) 698-709.

[6] S.C.M. Teixeira, High-pressure small-angle neutron scattering for food studies, Current Opinion in Colloid & Interface Science 42 (2019) 99-109.

[7] J.G.B. C. J. Glinka, B. Hammouda, S. Krueger, J.J. Moyer, W. J. Orts, The 30 m Small-Angle Neutron Scattering Instruments at the National Institute of Standards and Technology, J. Appl. Cryst. 31 (1998) 430-435.

[8] S.A. Ragland, A.K. Criss, From bacterial killing to immune modulation: Recent insights into the functions of lysozyme, PLoS Pathog 13(9) (2017) e1006512.

[9] Sasview for Small Angle Scattering Analysis - a SAS Community project. https://www.sasview.org/.

[10] B. Roig Solvas, D. Brooks, L. Makowski, Estimating the Anisotropy of Protein Structures from SAXS, 2018.

[11] J.B. Hayter, J. Penfold, An analytic structure factor for macroion solutions, Molecular Physics 42(1) (1981) 109-118.